Development/Plasticity/Repair

Mash1 and *Math3* Are Required for Development of Branchiomotor Neurons and Maintenance of Neural Progenitors

Ryosuke Ohsawa, Toshiyuki Ohtsuka, and Ryoichiro Kageyama
Institute for Virus Research, Kyoto University, Kyoto 606-8507, Japan

Basic helix–loop– helix (bHLH) transcription factors are known to play important roles in neuronal determination and differentiation. However, their exact roles in neural development still remain to be determined because of the functional redundancy. Here, we examined the roles of neural bHLH genes *Mash1* and *Math3* in the development of trigeminal and facial branchiomotor neurons, which derive from rhombomeres 2– 4. In *Math3*-null mutant mice, facial branchiomotor neurons are misspecified, and both trigeminal and facial branchiomotor neurons adopt abnormal migratory pathways. In *Mash1;Math3* double-mutant mice, trigeminal and facial branchiomotor neurons are severely reduced in number partly because of increased apoptosis. In addition, neurons with migratory defects are intermingled over the midline from either side of the neural tube. Furthermore, oligodendrocyte progenitors of rhombomere 4 are reduced in number. In the absence of *Mash1* and *Math3*, expression of Notch signaling components is severely downregulated in rhombomere 4 and neural progenitors are not properly maintained, which may lead to intermingling of neurons and a decrease in oligodendrocyte progenitors. These results indicate that *Mash1* and *Math3* not only promote branchiomotor neuron development but also regulate the subsequent oligodendrocyte development and the cytoarchitecture by maintaining neural progenitors through Notch signaling.

Key words: **bHLH; branchiomotor neuron; facial nucleus; hindbrain; Notch signaling; trigeminal nucleus**

Introduction

During vertebrate neural development, progenitors undergo proliferation and differentiation into neurons and glial cells, and these steps are regulated by multiple basic helix–loop–helix (bHLH) genes such as *Mash1* and *Neurogenin2* (for review, see Kageyama and Nakanishi, 1997; Lee, 1997; Bertrand et al., 2002; Ross et al., 2003). *Mash1* is expressed in the ventral telencephalon and regulates formation of GABAergic interneurons, whereas *Neurogenin2* is expressed in the dorsal telencephalon and regulates formation of glutamatergic pyramidal neurons (Casarosa et al., 1999; Horton et al., 1999; Fode et al., 2000; Parras et al., 2002; Schuurmans et al., 2004). In the developing retina, *Mash1* regulates bipolar cell development, whereas another bHLH gene, *NeuroD*, promotes amacrine cell genesis (Morrow et al., 1999; Hatakeyama et al., 2001; Inoue et al., 2002). Thus, distinct bHLH genes regulate distinct neuronal subtype specification. However, bHLH genes alone are not sufficient for generation of the neuronal diversity, but other types of transcription factor genes such as homeodomain genes are required. In the retina, the homeodomain gene *Chx10* regulates the layer identity, whereas *Mash1* determines the neuronal fate of the *Chx10*-specified layer (Hatakeyama et al., 2001).

Generation of the hindbrain neurons is also controlled by combinations of bHLH and homeodomain genes. The embryonic hindbrain is composed of reiterated segmental structures called rhombomeres. From each rhombomere, specific types of neurons are generated. For example, trigeminal branchiomotor neurons derive from rhombomere 2 (r2) and r3, whereas facial branchiomotor neurons derive from r4 (Marshall et al., 1992; Auclair et al., 1996; McKay et al., 1997; for review, see Chandrasekhar, 2004). These neurons migrate to the dorsolateral positions of the hindbrain. Recent studies revealed that *Mash1* regulates neurogenesis of the ventral r4 in combination with the homeodomain gene *Phox2b* (Dubreuil et al., 2002; Pattyn et al., 2004). In the absence of either *Mash1* or *Phox2b*, neurons are still generated, although they are misspecified and reduced in number in *Phox2b*-null embryos (Hirsch et al., 1998; Pattyn et al., 2000, 2003b), whereas in *Mash1;Phox2b* double-null embryos, neurons are completely missing (Pattyn et al., 2004). These results indicate that *Mash1* and *Phox2b* cooperatively promote neurogenesis in r4. However, it remains to be determined whether the homeodomain gene *Phox2b* alone can rescue all aspects of loss of *Mash1* or whether as yet unidentified bHLH genes may participate in the neurogenesis process. In the absence of *Phox2b*, expression of another bHLH gene, *Math3*, is lost (Pattyn et al., 2000), whereas misexpression of *Phox2b* induces *Math3* expression (Dubreuil et al., 2000), raising the possibility that *Math3* could compensate *Mash1* for some aspects of development of hindbrain neurons.

Received Nov. 10, 2004; revised April 11, 2005; accepted May 6, 2005.

This work was supported by the Sasagawa Research Grant from the Japan Scientific Society and research grants from the Ministry of Education, Culture, Sports, Science, and Technology of Japan. R.O. was supported by The 21st Century Center of Excellence Program of the Ministry of Education, Culture, Sports, Science, and Technology of Japan. We thank Dr. François Guillemot for *Mash1*-null mice and discussion. The monoclonal antibodies to Islet1 and Nkx2.2 were obtained from the Developmental Studies Hybridoma Bank (University of Iowa, Iowa City, IA).

Correspondence should be addressed to Dr. Ryoichiro Kageyama, Institute for Virus Research, Kyoto University, Shogoin-Kawahara, Sakyo-ku, Kyoto 606-8507, Japan. E-mail: rkageyam@virus.kyoto-u.ac.jp.

DOI:10.1523/JNEUROSCI.4621-04.2005

 0270-6474/05/255857-09$15.00/0

Here, we found that *Mash1* and *Math3* are transiently coexpressed by branchiomotor neuron progenitors. Furthermore, development of branchiomotor neurons is more severely affected in *Mash1;Math3* double-mutant embryos than in *Mash1*-null and *Math3*-null embryos. Our results indicate that *Mash1* and *Math3* cooperatively regulate development of trigeminal and facial branchiomotor neurons and maintenance of neural progenitors by activation of Notch signaling. Furthermore, in the absence of *Mash1* and *Math3*, oligodendrocyte development is affected because neural progenitors are not properly maintained.

Materials and Methods

Mouse strains. All animals used in this study were maintained and handled according to protocols approved by Kyoto University. Generation of *Mash1* and *Math3* mutant mice was reported previously (Guillemot et al., 1993; Tomita et al., 2000). Genotyping of mutants was performed by PCR. The primer sequences for genotyping of the *Mash1* mutant allele were as follows: 5′-ACGACTTGAACTCTATGGCGGGTTCTC-3′,5′-GCCACTCTCAGGGGCCAAGACTGAAGTTAA-3′, and 5′-AAATTAAGGGCCAGCTCATTCCTCCACTCA-3′. PCR products were loaded in a 1.5% agarose gel for electrophoresis. A 350 bp band indicates a wild-type allele, and a 280 bp band indicates a mutant allele. For genotyping of the *Math3* mutant allele, the primer sequences were 5′-GTATATGAAATCCAAGGACATGGTGGAGCT-3′, 5′-TGACTCTTCGAGCCCTGAATCTTTCAAGGC-3′, and 5′-CGCTGATCAGCCTCGACTGTGCCTTCTAGT-3′. A 260 bp band indicates a wild-type allele, and a 350 bp band indicates a mutant allele.

Immunohistochemistry. Embryos were fixed in 4% paraformaldehyde at 4°C for 3 h, washed in ice-cold PBS three times, equilibrated in 20% sucrose at 4°C, embedded in OCT compound, and frozen at −80°C. The sections were made by cryostat (Leica, Nussloch, Germany) at 16 μm thickness and incubated in 5% normal goat serum and 0.1% Triton X-100 at room temperature for 1 h, then incubated with primary antibodies against microtubule-associated protein 2 (MAP2; 1:1000; Sigma, St. Louis, MO), Nkx2.2 (1:200; 74.5A5; Hybridoma Bank, Iowa City, IA), Ki-67 (1:5000; BD PharMingen, San Diego, CA), N-cadherin (1:500; Transduction Laboratories, Lexington, KY), and Islet1 (1:200; 40.2; Hybridoma Bank). A biotinylated antibody against mouse IgG (1:200; Vector Laboratories, Burlingame, CA) was used for a secondary antibody. FITC-avidinD (1:1000; Vector Laboratories) was added to detect the signal.

In situ *hybridization. In situ* hybridization on tissue sections was performed as described previously (Hirata et al., 2001), using *Mash1*, *Math3*, *Hes5*, *Delta-like1*, *Delta-like3*, *Islet1*, *Sim1*, *c-Ret*, *Phox2b*, *Ebf-1*, *Sonic hedgehog* (*Shh*), and *neo* probes. RNA probes were labeled with digoxigenin. Embryos were dissected and fixed in 4% paraformaldehyde at 4°C overnight, rinsed with ice-cold PBS three times, equilibrated in 20% sucrose, embedded in OCT compound, and frozen at −80°C. Tissue sections were made by cryostat. The sections were treated with proteinase K, refixed with 0.2% glutaraldehyde and 4% paraformaldehyde, rinsed with 0.1% Tween 20 in PBS, and hybridized with RNA probe in 50% formamide, 5× SSC, 1% SDS, 50 μg/ml heparin, and 50 μg/ml tRNA solution at 65°C overnight. The sections were washed in 50% formamide, 5× SSC, and 1% SDS at 65°C, treated with ribonuclease, washed in 50% formamide and 2× SSC, washed in Tris-buffered saline, and incubated with alkaline phosphatase-conjugated antibody against digoxigenin at 4°C overnight. After incubation, the sections were washed with 0.1% Tween 20 in Tris-buffered saline three times, then in 100 mM NaCl, 100 mM Tris-HCl, pH 9.5, 50 mM $MgCl_2$, and 0.1% Tween 20 solution once. For a color development reaction, 4-nitroblue tetrazolium chloride and 5-bromo-4-chloro-3-indolyl phosphate (BCIP) were used as substrates.

For double RNA *in situ* hybridization, *Mash1* and *Math3* RNA probes were labeled with FITC and digoxigenin, respectively. Detection of *Math3* mRNA was performed as described above. After the first color development reaction, the sections were washed in Tris-buffered saline three times and incubated at 65°C to eliminate the alkaline phosphatase

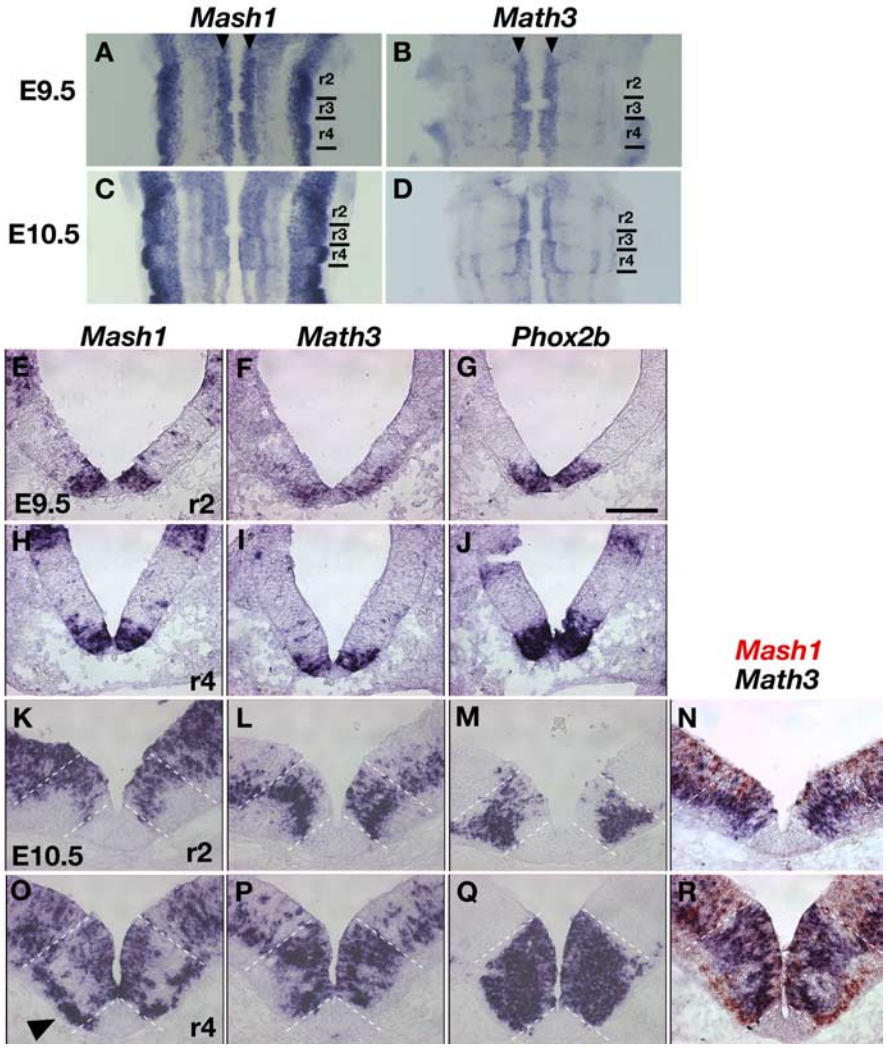

Figure 1. Expression patterns of *Mash1* and *Math3* in the developing hindbrain. *In situ* hybridization was performed for *Mash1* (***A***, ***C***, ***E***, ***H***, ***K***, ***O***, ***N***, ***R***), *Math3* (***B***, ***D***, ***F***, ***I***, ***L***, ***P***, ***N***, ***R***), and *Phox2b* (***G***, ***J***, ***M***, ***Q***). ***A–D***, The hindbrain was cut along the roof plate and flat mounted. At E9.5 and E10.5, *Mash1* was strongly expressed in the ventral hindbrain where trigeminal and facial branchiomotor neurons arise (***A***, arrowheads, ***C***). *Math3* was also expressed in the ventral hindbrain at E9.5 and E10.5 (***B***, arrowheads, ***D***). ***E–R***, *In situ* hybridization was performed with transverse sections through r2 (***E–G***, ***K–N***) and r4 (***H–J***, ***O–R***) at E9.5 (***E–J***) and E10.5 (***K–R***). In r2 and r4, which give rise to trigeminal and facial branchiomotor neurons, respectively, *Mash1* was expressed by subsets of ventricular cells as well as by cells migrating out of the ventricular zone (***E***, ***H***, between dashed lines in ***K***, ***O***). *Mash1* was also expressed in postmitotic inner-ear efferent neurons (***O***, arrowhead), as reported previously (Tiverson et al., 2003). *Math3* was expressed by cells in the ventricular zone as well as in the outer layers of r2 and r4 (***F***, ***I***, between dashed lines in ***L***, ***P***). *Phox2b* expression was well overlapped with *Mash1* and *Math3* expression domains in both r2 and r4 (***G***, ***J***, ***M***, ***Q***). At least some of the ventricular and migrating cells coexpressed *Mash1* and *Math3* (***N***, ***R***, between dashed lines). Scale bar, 100 μm.

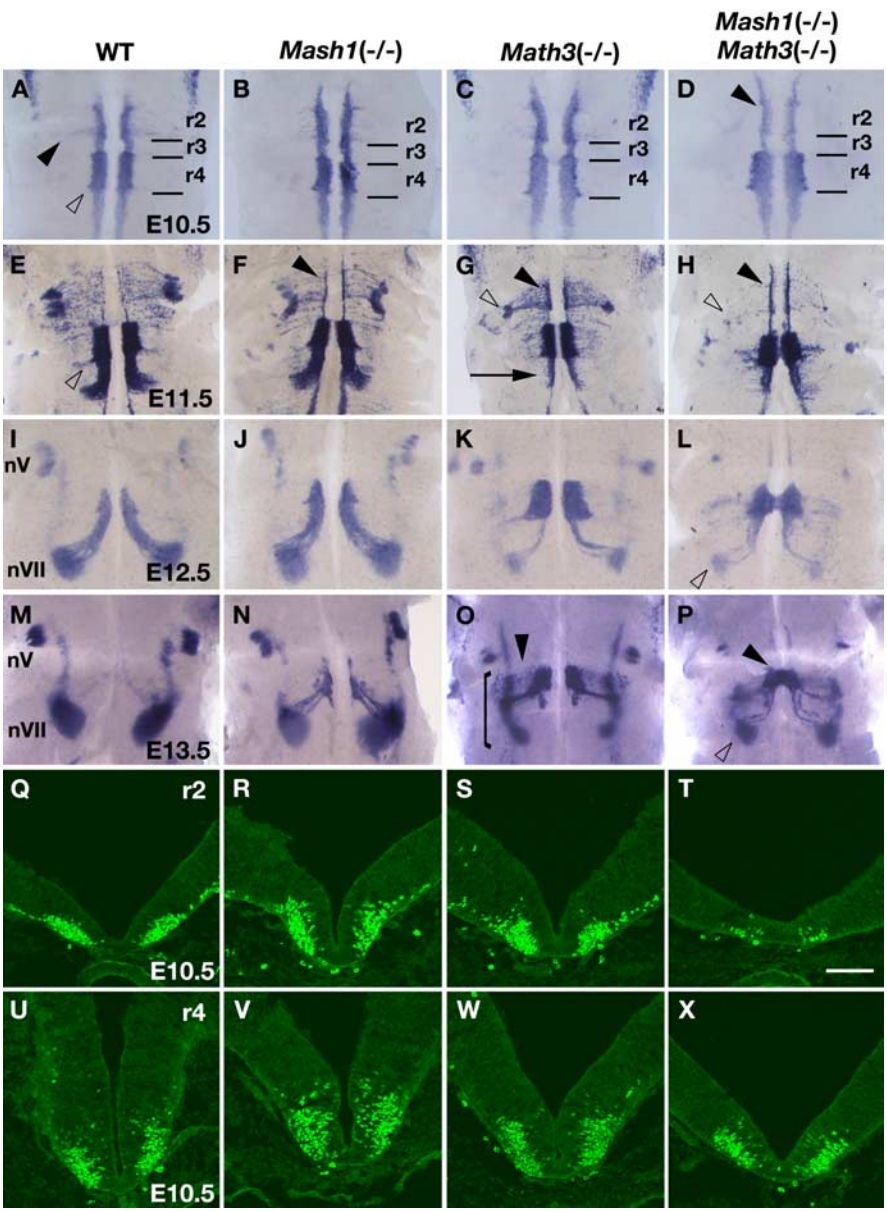

Figure 2. Developmental defects of trigeminal and facial branchiomotor neurons in mutant embryos. ***A–P***, *In situ* hybridization for *Islet1* was performed with the wild-type (***A***, ***E***, ***I***, ***M***), *Mash1*(−/−) (***B***, ***F***, ***J***, ***N***), *Math3*(−/−) (***C***, ***G***, ***K***, ***O***), and *Mash1*(−/−); *Math3*(−/−) (***D***, ***H***, ***L***, ***P***) hindbrain. The samples were cut along the roof plate and flat mounted. ***A–D***, At E10.5, trigeminal (***A***, filled arrowhead) and facial (***A***, open arrowhead) branchiomotor neurons (*Islet1* $^{+}$) were born in the ventral region of r2–r4 and started migration in the wild type. Similarly, these neurons were born in *Mash1*(−/−) (***B***) and *Math3*(−/−) (***C***). In *Mash1*(−/−); *Math3*(−/−), fewer neurons were born from r2 (***D***, arrowhead) than the others (***A–C***). ***E–H***, At E11.5, the majority of trigeminal branchiomotor neurons migrated to the dorsolateral position of r2 in the wild type and *Mash1*(−/−) (***E***, ***F***), although some neurons remained in the ventral region in *Mash1*(−/−) (***F***, arrowhead). Many of facial branchiomotor neurons migrated from r4 into r5 and r6 in the wild type (***E***, open arrowhead) and *Mash1*(−/−) (***F***). In *Math3*(−/−), many neurons still remained in r2 (***G***, filled arrowhead), resulting in a small nucleus (***G***, open arrowhead). Only subsets of r4 neurons migrated into r5 (***G***, arrow). In *Mash1*(−/−);*Math3*(−/−), most of the r2 neurons did not migrate (***H***, filled arrowhead), resulting in a very small trigeminal nucleus (***H***, open arrowhead). Only subsets of r4 neurons migrated into r5. ***I–L***, At E12.5, most trigeminal branchiomotor neurons finished migration, forming the trigeminal nucleus (nV) in the wild type and *Mash1*(−/−) (***I***, ***J***). Many of the facial branchiomotor neurons migrated into the dorsal region of r6, forming the facial nucleus (nVII) in the wild type and *Mash1*(−/−) (***I***, ***J***). In contrast, most facial branchiomotor neurons still remained in r4 in *Math3*(−/−) (***K***) and *Mash1*(−/−);*Math3*(−/−), resulting in a very small facial nucleus (***K***, ***L***, open arrowhead). In *Mash1*(−/−);*Math3*(−/−), r4 neurons were intermingled across the midline (***L***). ***M–P***, At E13.5, most facial branchiomotor neurons finished migration, forming the facial nucleus (nVII) in the wild type and *Mash1*(−/−) (***M***, ***N***). In contrast, in *Math3*(−/−), some facial branchiomotor neurons migrated within r4, forming an elongated nucleus (***O***, arrowhead and bracket). In *Mash1*(−/−);*Math3*(−/−), still many r4 neurons remained in the ventral r4, resulting in a small nucleus (***P***, open arrowhead). More neurons were intermingled across the midline (***P***, filled arrowhead). ***Q–X***, Immunohistochemistry against Islet1 was performed with transverse sections of r2 (***Q–T***) and r4 (***U–X***) at E10.5. Islet1 $^{+}$ cells were significantly reduced in number in *Mash1*(−/−); *Math3*(−/−) r2 (***T***). Scale bar, 100 μm. WT, Wild type.

activity for a primary reaction. The sections were then incubated with alkaline phosphatase-conjugated antibody against FITC at 4°C overnight. For the *Mash1* mRNA detection, 2-[4-iodophenyl]-3-[4-nitrophenyl]-5-phenyltetrazolium chloride and BCIP were used as substrates.

Whole-mount *in situ* hybridization was performed as described previously (Bessho et al., 2001) with the following minor modification. The hindbrain was dissected and cut at the dorsal edge of the neural tube before fixation. After performing whole-mount *in situ* hybridization, hindbrain tissues were flat mounted on a slide glass.

Terminal deoxynucleotidyl transferase-mediated dUTP nick end labeling assay. Embryos were dissected and fixed in 4% paraformaldehyde at 4°C for 3 h. After fixation, the embryos were rinsed with ice-cold PBS, equilibrated in 20% sucrose, embedded in OCT compound, and frozen at −80°C. The sections were made by cryostat at 16 μm thickness. Terminal deoxynucleotidyl transferase-mediated dUTP nick end labeling (TUNEL) assay was performed as indicated in the protocol provided by a manufacturer (*In Situ* Cell Death Detection kit; Roche, Mannheim, Germany).

Bromodeoxyuridine incorporation assay. Six hundred microliters of 10 mg/ml bromodeoxyuridine (BrdU) in PBS (6 mg) were injected intraperitoneally into pregnant mice. After 30 min, embryos were dissected and fixed in 4% paraformaldehyde at 4°C overnight. Then embryos were rinsed with ice-cold PBS three times, equilibrated in 20% sucrose, and embedded in OCT compound. The tissue sections were rinsed with PBS three times, blocked in 5% normal goat serum and 0.1% Triton X-100 at room temperature for 1 h, and treated with 2N HCl at 37°C for 30 min. After acidic treatment, the sections were neutralized in 0.1 M sodium tetraborate, pH 8.0, rinsed with PBS three times, and incubated with anti-BrdU antibody (1:1000; Sigma). Signal detection was performed as immunohistochemistry.

Results

Mash1 and *Math3* are expressed in branchiomotor neuron progenitors in the hindbrain

To characterize the roles of *Mash1* and *Math3* in hindbrain development, we first examined their expression patterns by *in situ* hybridization. The hindbrain was cut along the roof plate and flat mounted to locate the expression domains. At embryonic day 9.5 (E9.5), *Mash1* was expressed mainly in two longitudinal columns. Expression in the ventral column occurred at a high level from r2 to r4, where trigeminal and facial branchiomotor neurons arise (Fig. 1*A*, arrowheads). This expression continued but became less significant at E10.5 (Fig. 1*C*). *Math3* expression was also observed in the ventral column from r2 to r4 at E9.5 (Fig. 1*B*, arrowheads) and

continued at E10.5 (Fig. 1*D*). In r2 and r4, *Mash1* expression occurred mainly in the ventricular zone, whereas it continued in subsets of cells migrating out of the ventricular zone at both E9.5 and E10.5 (Fig. 1*E*,*H*,*K*,*O*). *Math3* expression also occurred in the ventricular zone, but *Math3* was expressed mainly by the cells in the outer layers of r2 and r4 during this period (Fig. 1*F*,*I*,*L*,*P*). Some of these cells coexpressed *Mash1* and *Math3* (Fig. 1*N*,*R*). These results suggest that *Mash1* and *Math3* are expressed by both neural progenitors and differentiating neurons of r2 to r4.

Because the ventral region of r2–r4 is known to give rise to branchiomotor neurons, we next compared the expression patterns of *Mash1* and *Math3* with those of *Phox2b*, which has been shown to control branchiomotor neuron generation (Pattyn et al., 1997, 2000). *Phox2b* expression was well overlapped with the *Mash1* and *Math3* expression domains in r2 and r4 (Fig. 1*G*,*J*, between dashed lines in *M*,*Q*). These results suggest that *Mash1* and *Math3* are expressed at distinct but overlapping stages by differentiating trigeminal and facial branchiomotor neurons and their progenitors.

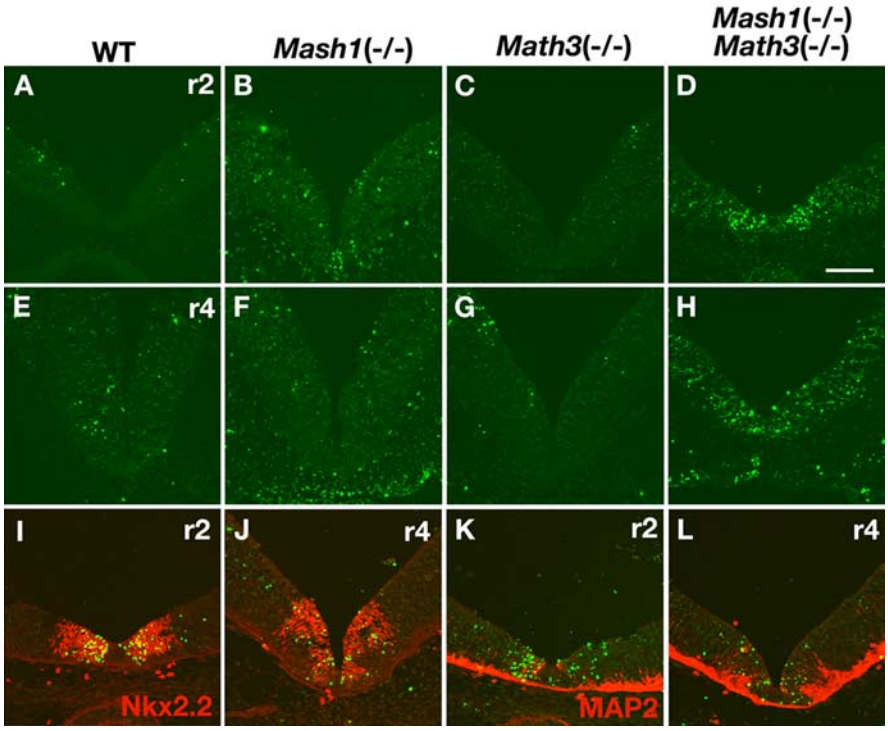

Figure 3. Increased apoptosis in *Mash1(−/−);Math3(−/−)* hindbrain. TUNEL assay was performed with transverse sections of r2 (***A–D***, ***I***, ***K***) and r4 (***E–H***, ***J***, ***L***) at E10.5. More cells died in r2 and r4 of *Mash1(−/−);Math3(−/−)* (***D***, ***H–L***). These apoptotic cells expressed Nkx2.2 (***I***, ***J***) but not MAP2 (***K***, ***L***), suggesting that double-mutant cells undergo apoptosis before becoming mature neurons (***I–L***). Apoptotic cells were also slightly increased in number in *Mash1*(−/−) r2 (***B***). Scale bar, 100 μm. WT, Wild type.

Defects of trigeminal branchiomotor neuron development in *Math3(−/−)* and *Mash1(−/−);Math3(−/−)* mutants

To investigate the roles of *Mash1* and *Math3* in branchiomotor neuron development, we first analyzed trigeminal motor neurons in *Mash1*-null and/or *Math3*-null mice. We used *Islet1* as a general motor neuron marker (Ericson et al., 1992). In wild-type embryos, trigeminal branchiomotor neurons arose from the ventral region of r2 and r3 between E9.5 and E10.5 (Taber Pierce, 1973; Marshall et al., 1992) and migrated dorsolaterally to form the trigeminal motor nucleus (Fig. 2*A*, arrowhead, *Q*) (Altman and Bayer, 1982), which extended in the dorsolateral position of r2 and r3. This migration was almost completed by E11.5, and only a few motor neurons remained in the ventral region (Fig. 2*E*). Although trigeminal motor neurons appeared to be generated normally in *Mash1*-null embryos (Fig. 2*B*,*F*,*R*), a few more motor neurons still remained in the ventral region adjacent to the floor plate of r2 and r3 at E11.5 (Fig. 2*F*, arrowhead), suggesting that the development of trigeminal branchiomotor neurons is slightly delayed compared with the wild type. Similarly, more motor neurons remained in the ventral region of r2 and r3 at E11.5 in *Math3*-null embryos (Fig. 2*G*, filled arrowhead), although trigeminal motor neurons were normally born at E10.5 (Fig. 2*C*,*S*). In addition, the trigeminal motor nucleus of *Math3*-null embryos was smaller than that of the wild type (Fig. 2*G*, open arrowhead). This is likely attributable to a migratory defect, because more neurons remained in the ventral region of *Math3* mutants (Fig. 2*G*, filled arrowhead). Furthermore, the rostral neurons migrated dorsocaudally to converge on a small caudal nucleus in r2 (Fig. 2*G*, open arrowhead). These results indicate that *Math3* is important for migratory behavior of trigeminal branchiomotor neurons.

Because the overlapping patterns of *Mash1* and *Math3* expression suggest redundant roles of these bHLH genes, we next examined *Mash1;Math3* double-mutant embryos. In the double mutants, trigeminal motor neurons were severely reduced in number at E10.5 and E11.5 (Fig. 2*D*,*H*, filled arrowhead, *T*). Very few cells migrated dorsolaterally, and, as a result, the trigeminal motor nucleus was very small at E11.5 (Fig. 2*H*, open arrowhead) compared with the wild type, *Mash1*-null, and *Math3*-null embryos (Fig. 2*E–G*). At later stages, the trigeminal motor nucleus (nV) was also very small (Fig. 2*L*,*P*). To further investigate the cause of the defects of the double-mutant embryos, we examined apoptotic cell death by TUNEL assay. In wild-type embryos and *Math3*-null embryos, no overt apoptotic cell death was observed in r2 (Fig. 3*A*,*C*), whereas a few TUNEL-positive cells were detected in *Mash1*-null embryos (Fig. 3*B*). In contrast, TUNEL-positive cells were significantly increased in r2 of *Mash1;Math3* double-mutant embryos (Fig. 3*D*). These apoptotic cells expressed Nkx2.2 (Fig. 3*I*) but were negative for the neuronal marker MAP2 (Fig. 3*K*), suggesting that cells undergo apoptosis before becoming mature neurons in the absence of *Mash1* and *Math3*. These results indicate that *Mash1* and *Math3* are required for migration and survival of immature trigeminal branchiomotor neurons.

Defects of facial branchiomotor neuron development in *Math3* and the double mutants

We next examined development of facial branchiomotor neurons in mutant embryos. Facial branchiomotor neurons are known to adopt unique migratory pathways (Garel et al., 2000). In wild-type embryos, facial branchiomotor neurons arose at r4 from E9.5–E11.5 (Fig. 2*A*,*E*, open arrowheads, *U*) (McKay et al.,

1997; Pattyn et al., 2003b). After E10.5, they migrated caudally, keeping its position adjacent to the floor plate. After entering r6, they switched the direction and migrated dorsolaterally, forming the nucleus at r6 (Fig. 2*I*,*M*, nVII). This migration was almost completed at E14.5. In *Mash1* mutant embryos, generation and migration of facial branchiomotor neurons seemed to be normal at E10.5–E12.5 (Fig. 2*B*,*F*,*J*,*V*). However, at E13.5, many cells still remained near the floor plate of r4 or on the way to r6 (Fig. 2*N*), although some of them in r4 could be aberrant inner-ear efferent neurons (Tiveron et al., 2003). These results suggest that in the absence of *Mash1*, facial branchiomotor neurons exhibit a delay of migration. However, at later stages, the facial motor nucleus was formed, and no overt defect was observed (data not shown). In contrast, *Math3*-null embryos exhibited abnormal migration of facial branchiomotor neurons. At E11.5, very few cells reached r6 (Fig. 2*G*, arrow), whereas the majority of the cells remained in the ventral region of r4 of *Math3*-null embryos (Fig. 2*G*). At E12.5, very few cells reached the dorsolateral position of r6, whereas the majority still remained in the ventral region of r4 (Fig. 2*K*). At E13.5, in *Math3*-null embryos, some of these neurons migrated dorsolaterally within r4 (Fig. 2*O*, arrowhead), forming an elongated nucleus between r4 and r6 (Fig. 2*O*, bracket), in contrast to the wild-type facial motor nucleus, which resided in r6 (Fig. 2*M*).

In the *Mash1;Math3* double-mutant hindbrain, although many neurons were born in the ventral r4 at E10.5 (Fig. 2*D*,*X*), very few cells reached r6 at E11.5, whereas the majority of the cells remained in the ventral region of r4 (Fig. 2*H*). At E12.5 and E13.5, only subsets of cells reached the dorsolateral position of r6 (Fig. 2*L*,*P*, open arrowheads), whereas other subsets migrated within r4, forming an elongated nucleus between r4 and r6, which is similar to but smaller than the *Math3*-null nucleus (Fig. 2*O*,*P*). In *Mash1;Math3* double-mutant r4, TUNEL-positive cells were increased (Fig. 3*H*) compared with the others (Fig. 3*E*–*G*). These apoptotic cells expressed Nkx2.2 (Fig. 3*J*) but were negative for the neuronal marker MAP2 (Fig. 3*L*), suggesting that cells undergo apoptosis before becoming mature neurons in the absence of *Mash1* and *Math3*. These results indicate that *Mash1* and *Math3* are required for migration and survival of immature facial branchiomotor neurons. Strikingly, the left and right neurons, which are normally separated by the floor plate, were fused across the midline in r4 of the double mutants. This fusion started at E12.5 (Fig. 2*L*) and became more severe at E13.5 (Fig. 2*P*, arrowhead). Thus, in the absence of *Mash1* and *Math3*, the cytoarchitecture of r4 was disrupted.

Misspecification of facial branchiomotor neurons in *Math3* mutant embryos

To characterize the migratory defects of facial branchiomotor neurons in *Math3* mutant mice, we examined several markers that are expressed during migration. Expression of *c-Ret*, a gene for the glial cell line-derived neurotrophic factor receptor, initiates in facial branchiomotor neurons only after they migrate into r5 (Garel et al., 2000). In the wild-type embryos, few, if any, cells expressed *c-Ret* at E10.5 (Fig. 4*A*). In contrast, in *Math3* mutant embryos, *c-Ret* expression occurred ectopically in r4 (Fig. 4*B*), suggesting that this ectopic expression may affect migration of branchiomotor neurons. *Sim1*, a gene for a bHLH-PAS (motif of proteins PER-ARNT-SIM) transcription factor expressed by V3 interneurons of the spinal cord (Fan et al., 1996; Briscoe et al., 1999), was not expressed in the wild-type hindbrain (Fig. 4*C*). In contrast, *Sim1* was ectopically expressed in the ventral region of r4 of *Math3*(−/−) at E11.5 (data not shown) and E13.5 (Fig. 4*D*). These results indicate that facial branchiomotor neurons are misspecified in *Math3* mutant embryos, raising the possibility that this misspecification may lead to the migratory defect of these neurons.

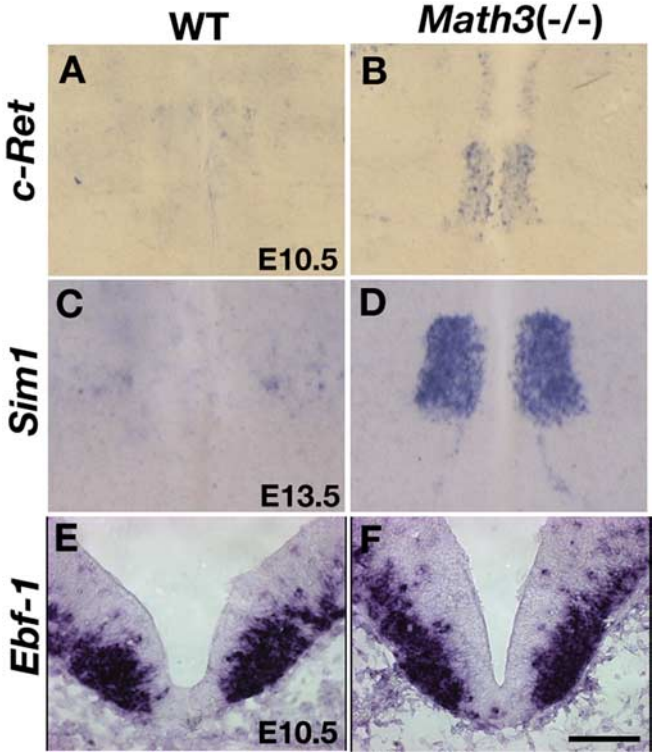

Figure 4. Ectopic gene expression in *Math3*(−/−) hindbrain. *In situ* hybridization for *c-Ret* (***A***, ***B***), *Sim1* (***C***, ***D***), and *Ebf-1* (***E***, ***F***) was performed with flat-mounted hindbrain (***A–D***) and transverse (***E***, ***F***) sections of r4 at the indicated time points. ***A***, ***B***, *c-Ret* expression was rarely detectable in the wild type although ectopically upregulated in the ventral r4 of *Math3*(−/−). ***C***, ***D***, *Sim1* expression was not detected in the wild type but occurred at a high level in the ventral r4 of *Math3*(−/−). Thus, branchiomotor neurons of r4 were misspecified in *Math3*(−/−). ***E***, ***F***, *Ebf-1*, which is required for migration of branchiomotor neurons, was not significantly affected in *Math3* mutant embryos, suggesting that *Ebf-1* is not involved in the migratory defects of *Math3* mutant facial branchiomotor neurons. Scale bar: (in ***F***) ***E***, ***F***, 100 μm. WT, Wild type.

In contrast, expression of the bHLH gene *Ebf-1*, which is required for correct migration of branchiomotor neurons (Garel et al., 2000), was not significantly affected in *Math3* mutant embryos (Fig. 4*E*,*F*). Thus, these *Math3*-null cells are not totally transformed into other cell types, although they are severely misspecified.

Loss of neural progenitors in the ventral region of *Mash1; Math3* double-mutant r4

In the absence of *Mash1* and *Math3*, facial branchiomotor neurons on either side were fused across the midline in r4. To examine this fusion, we made transverse sections through r4 at E13.5. In the wild type, the inner surface was covered by the MAP2-negative ventricular zone, which contains neural progenitors (Fig. 5*A*). In contrast, in the ventral region of the double-mutant r4, the ventricular cells were missing and instead MAP2-positive neurons from either side of the neural tube were fused together over the floor plate (Fig. 5*B*, boxed region). Furthermore, these MAP2-positive neurons were exposed directly to the fourth ventricle (Fig. 5*B*′). Neural progenitors are known to have the tight junction and adherens junction at the apical side and thereby prevent neurons from migrating into the ventricular lumen: premature loss of neural progenitors leads to intermingling of neu-

rons from the left and right walls of the neural tube (Hatakeyama et al., 2004). In the wild type, the adherens junction molecule N-cadherin was highly expressed at the apical surface (Fig. 5*C*), whereas it was missing in the double mutants (Fig. 5*D*, arrowheads), suggesting that neural progenitors are prematurely lost. In agreement with this observation, BrdU uptake and expression of Ki-67, a marker for mitotic cells, were reduced in the double mutants compared with the wild type as early as E10.5 (Fig. 5*E–H*), indicating that dividing neural progenitors are not properly maintained in the absence of *Mash1* and *Math3*. The floor plate, which expresses Shh, was maintained in the double mutants as in the wild type at both E10.5 and E13.5 (Fig. 5*I–L*), indicating that the midline structure is not lost in the double mutants. Thus, inactivation of *Mash1* and *Math3* is likely to lead to premature loss of neural progenitors and their apical junctional complex and thereby allows facial branchiomotor neurons to intermingle each other from either side of the neural tube. This observation implies that *Mash1* and *Math3* are required not only for normal development of branchiomotor neurons but also for maintenance of neural progenitors and the cytoarchitecture.

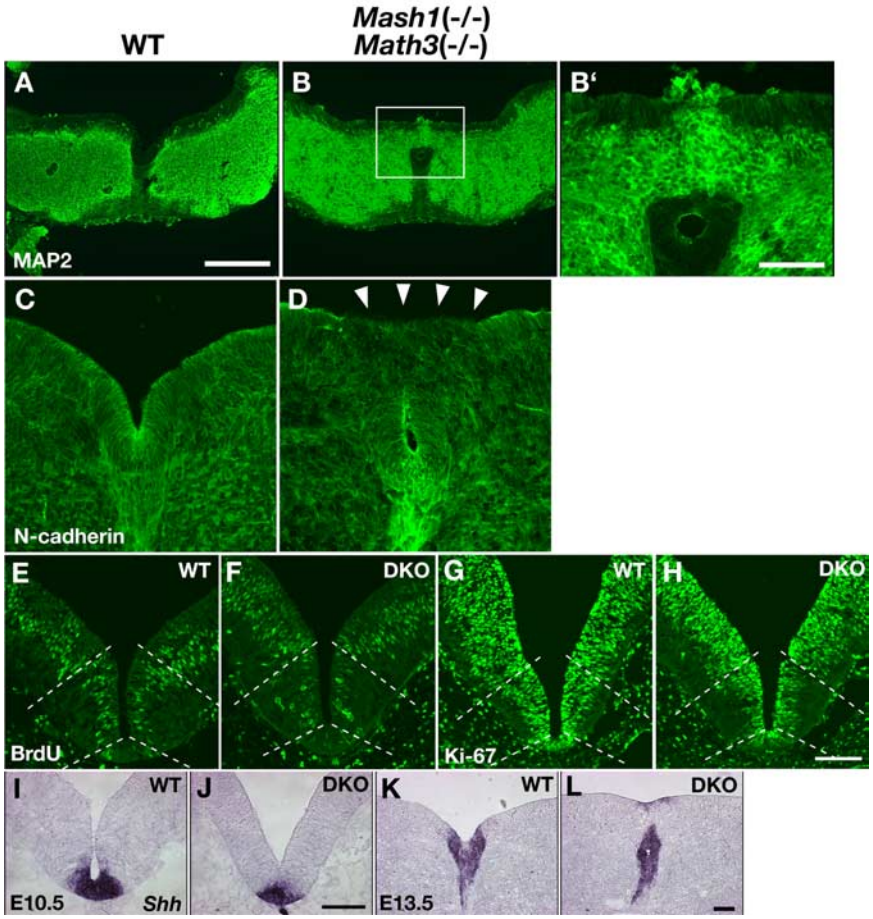

Figure 5. Intermingling of r4 neurons across the midline in *Mash1(−/−);Math3(−/−)*. Transverse sections of the ventral r4 were examined. ***A***, ***B***, ***B′***, In the wild type, the inner surface of the hindbrain was covered by MAP2-negative ventricular cells, and neurons (MAP2 $^{+}$) were not present in the midline region at E13.5 (***A***). In contrast, many neurons were intermingled across the midline in *Mash1(−/−);Math3(−/−)* (***B***). The boxed region in ***B*** is enlarged in ***B′***. Intermingled neurons were exposed to the lumen of the hindbrain. ***C***, ***D***, The adherens junction molecule N-cadherin was highly expressed at the apical side in the wild type (***C***), whereas it was missing in the double mutants (***D***, arrowheads). ***E***, ***F***, BrdU uptake was examined at E10.5. BrdU uptake was reduced in the double mutants (***F***) compared with the wild type (***E***). ***G***, ***H***, Ki-67 expression was examined by immunohistochemistry at E10.5. Ki-67 expression was reduced in the double mutants (***H***) compared with the wild type (***G***). ***I–L***, *In situ* hybridization of *Shh*. *Shh* was expressed in both the wild-type and double-mutant floor plate at E10.5 and E13.5. Scale bars: (in ***A***) ***A***, ***B***, 400 μm; ***B′***, 100 μm; ***E–L***, 100 μm. WT, Wild type; DKO, double knock-out.

Notch signaling is impaired in *Mash1(−/−);Math3(−/−)* double-mutant mice

Because Notch signaling is known to regulate maintenance of neural progenitors (Ohtsuka et al., 1999; Gaiano et al., 2000; Hitoshi et al., 2002), we next addressed whether Notch signaling is affected in the double-mutant embryos. We first examined expression of *Hes5*, a downstream Notch effector (Ohtsuka et al., 1999). In the ventral r4 of the wild-type, *Mash1*(−/−), and *Math3*(−/−) embryos, expression of *Hes5* was observed at E10.5 (Fig. 6*A–C*). In contrast, in the double-mutant r4, *Hes5* expression was significantly downregulated (Fig. 6*D*, between dashed lines). At E11.5, *Hes5* expression remained at a very low level in the double mutants, whereas *Hes5* expression was still maintained in the wild-type, *Mash1*-null, and *Math3*-null r4 (Fig. 6*E–H*), although it was also slightly downregulated in *Mash1*-null r4 (Fig. 6*F*). These results indicate that Notch signaling is affected in the double-mutant embryos, which accounts for loss of neural progenitors.

Because neuronal bHLH genes are known to activate expression of Notch ligands such as Delta, we next examined expression of *Delta-like1* (*Dll1*) and *Dll3*. In the wild-type and *Math3*(−/−) embryos, *Dll1* expression occurred at E10.5 and E11.5 in the ventral domain where facial motor neurons are generated, whereas it was slightly decreased in *Mash1*(−/−) embryos (Fig. 6*I–K*,*M–O*). In contrast, in the double mutants, *Dll1* expression in the ventral r4 was downregulated at E10.5 (Fig. 6*L*) and mostly missing at E11.5 (Fig. 6*P*). Similarly, expression of *Dll3* was missing in the double mutants at E10.5 (Fig. 6*T*, between dashed lines), in contrast to the wild-type, *Mash1*-null, and *Math3*-null embryos (Fig. 6*Q–S*). Thus, expression of the Notch ligands is also lost in the absence of *Mash1* and *Math3*, which is likely to lead to downregulation of *Hes5* in neighboring cells.

The loss of Notch ligand expression could be attributable to either downregulation of the gene expression in cells that should normally express *Mash1/Math3* or apoptotic loss of these cells. To differentiate between these possibilities, we monitored *Mash1/Math3*-expressing cells in the double-mutant hindbrain. In *Mash1* and *Math3* mutant alleles, a neomycin-resistant (*neo*) gene cassette was inserted into each locus in the same and reverse orientations, respectively (Guillemot et al., 1993; Tomita et al., 2000). Thus, we could use the *neo* antisense and sense strand probes as an indicator for the *Mash1* and *Math3* promoter activities, respectively. In the wild-type embryos, *Math3* was expressed by cells adjacent to the floor plate of r4 at E11.5 (Fig. 7*A*, arrow). In the double-mutant embryos, the antisense *neo* was expressed in the same domain (Fig. 7*B*, arrow). Similarly, the sense *neo* was expressed in the same domain (Fig. 7*D*). Thus, the cells that should normally express *Mash1*/*Math3* did not die but still ex-

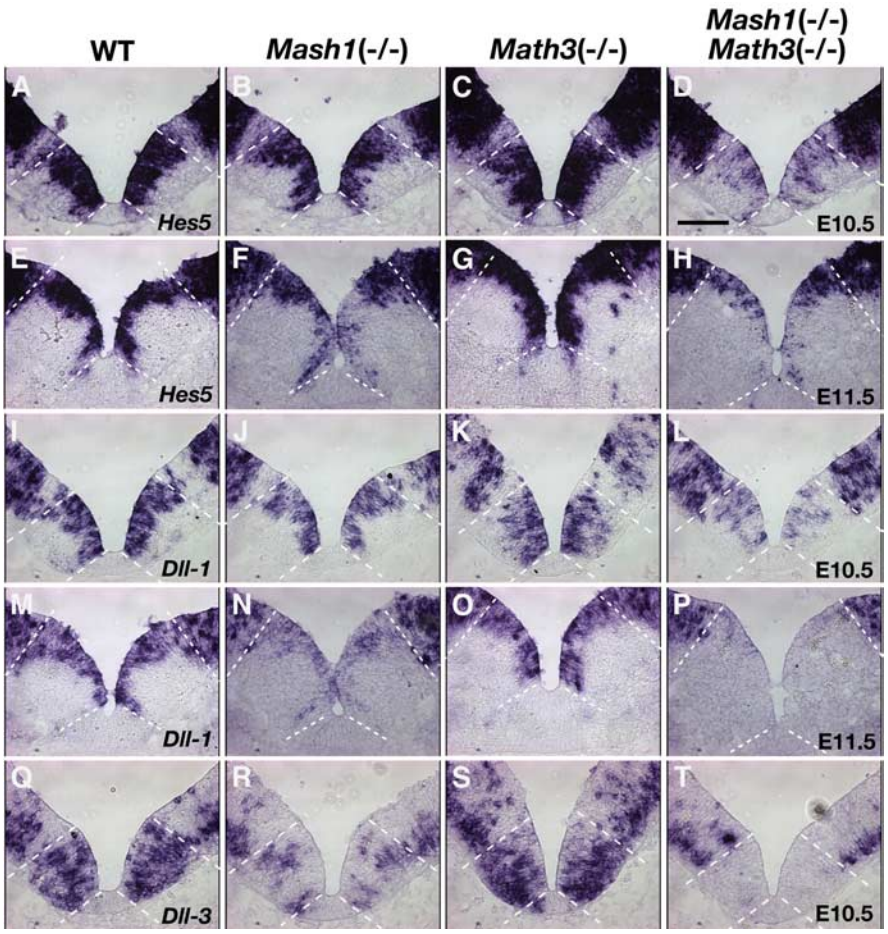

Figure 6. Impairment of Notch signaling in the ventral r4 of *Mash1(−/−);Math3(−/−)*. *In situ* hybridization for *Hes5* (***A–H***), *Dll1* (***I–P***), and *Dll3* (***Q–T***) was performed with transverse sections of the ventral r4 at E10.5 (***A–D***, ***I–L***, ***Q–T***) and E11.5 (***E–H***, ***M–P***). In *Mash1(−/−);Math3(−/−)*, expression of *Hes5* (***D***, ***H***), *Dll1* (***L***, ***P***), and *Dll3* (***T***) was significantly downregulated in the ventral r4, which gives rise to facial branchiomotor neurons (between dashed lines). In *Mash1*(−/−), expression of *Hes5* (***B***, ***F***), *Dll1* (***J***, ***N***), and *Dll3* (***R***) was slightly downregulated compared with the wild type and *Math3*(−/−). Scale bar, 100 μm. WT, Wild type.

isted in the double-mutant embryos at E11.5, indicating that loss of *Dll1* and *Dll3* expression is attributable to downregulation of the gene expression rather than to cell death.

We also noted that antisense *neo*-positive cells were present in a higher density in the double-mutant ventricular zone than in the wild type, which exhibited a salt-and-pepper pattern (Fig. 7, compare arrows in *A*, *B*). This is probably because Notch signaling, which represses neuronal bHLH gene expression of neighboring cells in a way known as "lateral inhibition," is impaired in the double mutants.

The delay of oligodendrocyte development in *Mash1(−/−); Math3(−/−)* mouse embryos

The ventral region is known to give rise to oligodendrocytes after generating motor neurons. Because neural progenitors were significantly decreased in the double mutants, we next examined the development of oligodendrocytes in the ventral r4 of the double mutants. In r4, expression of the early oligodendrocyte marker *PDGFRα* was observed at E12.5 in the wild-type, *Mash1*(−/−) and *Math3*(−/−) embryos (Fig. 8*A–C*). In contrast, in *Mash1(−/−);Math3(−/−)* embryos, *PDGFRα*-positive cells were severely reduced in number (Fig. 8*D*). These results suggest that impairment of maintenance of neural progenitors may lead to reduction of oligodendrocyte progenitors. At E14.5, however, *PDGFRα*-positive cells were found to be distributed throughout the hindbrain in the double-mutant embryos (data not shown). Thus, development of oligodendrocytes is not dependent on *Mash1* or *Math3*, and the initial decrease of oligodendrocyte progenitors can be recovered at later stages.

Discussion

Mash1 and *Math3* cooperatively regulate development of trigeminal and facial branchiomotor neurons

We found here that *Mash1* and *Math3* cooperatively regulate development of trigeminal and facial branchiomotor neurons. In the absence of *Mash1* and *Math3*, these neurons exhibit migratory defects and apoptosis, resulting in formation of very small trigeminal and facial nuclei. Furthermore, in r4, neurons with migratory defects are intermingled over the midline from either side of the neural tube, and oligodendrocyte progenitors are reduced in number. Thus, *Mash1* and *Math3* not only promote branchiomotor neuron development but also regulate the subsequent oligodendrocyte development and the cytoarchitecture in the hindbrain. It has been shown that neurons derived from the ventral r4 are completely missing in *Mash1;Phox2b* double-null embryos, whereas they are still generated in *Mash1*-null and *Phox2b*-null embryos, indicating that *Mash1* and *Phox2b* cooperatively promote neurogenesis in the ventral r4 (Pattyn et al., 2004). However, because *Phox2b* upregulates *Math3* expression (Dubreuil et al., 2000, 2002; Pattyn et al., 2000), our present data raise the possibility that at least some aspects of *Phox2b* functions in rescuing *Mash1* activities are mediated by *Math3*. Particularly, apoptosis and decrease of expression of Notch signaling molecules observed in *Mash1*-null mice are more severely affected in *Mash1;Math3* double-null mice, indicating that *Math3* may compensate *Mash1* for cell survival and activation of Notch signaling.

Mash1 and *Math3* function at a neuronal differentiation process in the hindbrain

Our present study established the roles of *Mash1* and *Math3* in the differentiation process of cranial branchiomotor neurons. In the double mutants, although trigeminal and facial branchiomotor neurons seemed to be born normally, they underwent cell death at E10.5. As a result, expression of the neuronal markers MAP2 and β-tubulin III exhibited marked reduction (data not shown). Furthermore, the majority of the surviving neurons did not properly migrate but remained in the ventral region, where they were born. Thus, in the absence of *Mash1* and *Math3*, the neuronal fate seems to be determined, but the subsequent differentiation process is impaired, although *Mash1* and *Math3* are known to regulate the neuronal fate determination process. It is possible that other bHLH genes may compensate for the deter-

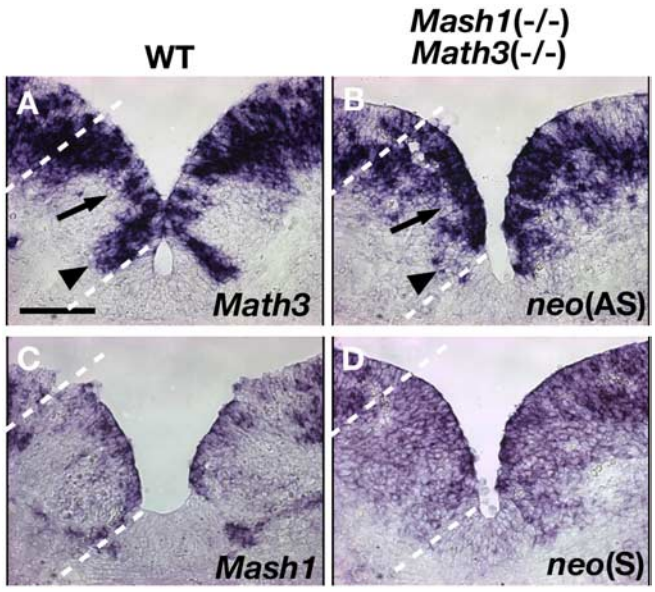

Figure 7. The cells that should normally express *Mash1* and *Math3* remained in *Mash1(−/−); Math3(−/−)*. *In situ* hybridization was performed with transverse sections of the ventral r4 at E11.5. ***A***, *Math3* was expressed in a salt-and-pepper pattern in the ventral r4 of the wild type (arrow). ***B***, Expression of the antisense neomycin mRNA under the control of the *Math3* promoter was detected in the ventral r4 of *Mash1(−/−); Math3(−/−)* (between dashed lines). ***C***, *Mash1* was expressed in the ventral r4 of the wild type. ***D***, Expression of the sense neomycin mRNA under the control of the *Mash1* promoter was detected in the ventral r4 of *Mash1(−/−); Math3(−/−)* (between dashed lines). Thus, the cells that should normally express *Mash1/Math3* remained in the double mutants. Cells adjacent to the floor plate were decreased in the double mutants (compare arrowheads in ***A***, ***B***). Scale bar, 100 μm. WT, Wild type.

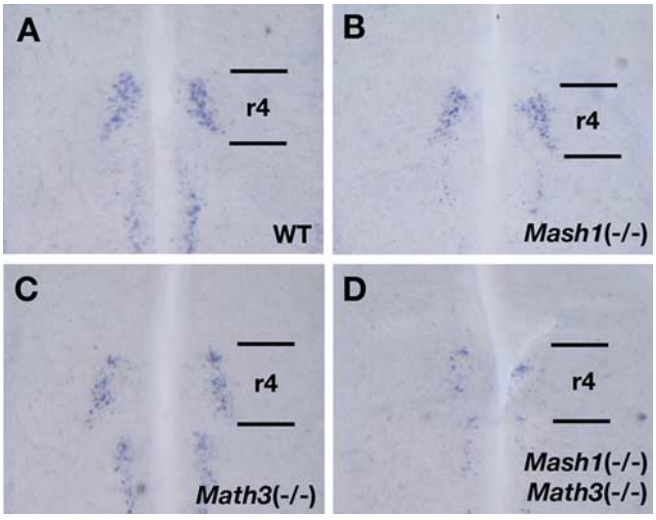

Figure 8. Impairment of oligodendrocyte development in the ventral r4 of *Mash1(−/−); Math3(−/−)*. *In situ* hybridization for *PDGFRα* was performed at E12.5. *PDGFRα* expression was significantly downregulated in the ventral r4 of *Mash1(−/−); Math3(−/−)* (***D***) compared with the others (***A–C***). Thus, oligodendrocyte progenitors were significantly reduced in number in the double mutants. WT, Wild type.

mination step. Alternatively, *Phox2b* itself has neuronal fate determination activities, as described previously (Dubreuil et al., 2000; Pattyn et al., 2004), although it remains to be determined whether *Phox2b* can directly activate the neuronal fate determination program without inducing neuronal bHLH gene expression.

Mash1 and *Math3* regulate Notch ligand expression in r4

It was reported previously that *Dll1* expression is completely lost in r4 of *Phox2b;Mash1* double-mutant embryos. This loss of *Dll1* expression in *Phox2b;Mash1* double mutants is probably as a result of the complete blockade of neurogenesis (Pattyn et al., 2004). In the present study, we showed that *Dll1* and *Dll3* expression is also lost in the ventral r4 of the *Mash1;Math3* double mutants, although many neurons are born. It is thus likely that *Mash1* and *Math3* cooperatively maintain Notch ligand expression in these neurons and thereby activate Notch signaling and downregulate *Mash1* and *Math3* expression in neighboring cells, resulting in a salt-and-pepper expression pattern. Consistent with this idea, in the absence of *Mash1* and *Math3*, expression of the Notch effector *Hes5* is lost, and the *Mash1* and *Math3* promoter activities are uniformly upregulated in the double-mutant ventricular cells. Our results thus suggest that *Math3*, rather than *Phox2b*, directly regulates Notch ligand expression in collaboration with *Mash1*.

Control of facial branchiomotor neuron migration

Facial branchiomotor neurons adopt a unique migratory pathway, and we found that in the absence of *Math3*, this migration is severely affected. Thus far, it has been shown that facial branchiomotor neuron progenitors and their progeny start expression of the three transcription factor genes *Nkx6.1*, *Math3*, and *Ebf-1* in this order, and mutant analyses revealed that each gene is required for the normal migration. In the absence of the earliest onset gene *Nkx6.1*, facial branchiomotor neurons migrate dorsolaterally within r4, forming the nucleus mainly in r4 (Müller et al., 2003; Pattyn et al., 2003a), whereas in the absence of the latest onset gene *Ebf-1*, dorsolateral migration occurs in r5–r6, forming the nucleus in r5–r6 (Garel et al., 2000). In the absence of the intermediate onset gene *Math3*, some populations of facial branchiomotor neurons exhibit aberrant migration in r4–r5, whereas others exhibit normal migration within r6, forming an elongated nucleus extending from r4 to r6. Thus, inactivation of *Nkx6.1*, *Math3*, and *Ebf-1* allows migration of branchiomotor neurons in r4, r4–r6, and r5–r6, respectively, in contrast to the wild type allowing dorsal migration only in r6. The onset of aberrant migration correlates well with the onset of gene expression, indicating that each gene prevents ectopic migration in a stage-specific manner. It is thus likely that the behavior of facial branchiomotor neurons should be controlled strictly by *Nkx6.1*, *Math3*, and *Ebf-1* in this order and, in their absence, these neurons could prematurely undergo dorsolateral migration.

c-Ret is prematurely expressed by Math3-null branchiomotor neurons in r4, as observed in *Ebf-1* mutants, and this ectopic *c-Ret* expression probably accounts for the aberrant dorsal migration of these neurons. Although *Mash1* and *Math3* are functionally redundant in the branchiomotor neuron development as shown above, most of the migratory defects are attributable only to *Math3* mutation, indicating that *Math3* has a unique role in migration of branchiomotor neurons.

Maintenance of neural progenitors by *Mash1* and *Math3*

We showed that oligodendrocyte progenitors are reduced in number at E12.5 in *Mash1;Math3* double mutants, although the number of oligodendrocytes becomes comparable with that of the wild-type embryos at E14.5. This recovery is probably because of the highly proliferative property of oligodendrocyte progenitors, as shown in the analysis of *Pax6* mutant mice (Sun et al., 1998). The reduction of oligodendrocyte progenitors at E12.5 in the double mutants is likely attributable to decrease of neural

progenitors because Notch signaling is impaired. Another interesting observation is intermingling of branchiomotor neurons across the midline in the double mutants. This defect is also likely attributable to loss of neural progenitors. Because neural progenitors have the tight and adherens junctions at the apical side to prevent neurons from scattering, premature loss of neural progenitors allows neurons to escape into the lumen (Hatakeyama et al., 2004). Thus, *Mash1* and *Math3* play an important role in maintenance of neural progenitors to ensure not only a sufficient supply of glial progenitors but also the structural integrity of the nervous system.

References

Altman J, Bayer SA (1982) Development of the cranial nerve ganglia and related nuclei in the rat. Adv Anat Embryol Cell Biol 74:1–90.

Auclair F, Valdes N, Marchand R (1996) Rhombomere-specific origin of branchial and visceral motoneurons of the facial nerve in the rat embryo. J Comp Neurol 369:451–461.

Bertrand N, Castro DS, Guillemot F (2002) Proneural genes and the specification of neural cell types. Nat Rev Neurosci 3:517–530.

Bessho Y, Sakata R, Komatsu S, Shiota K, Yamada S, Kageyama R (2001) Dynamic expression and essential functions of Hes7 in somite segmentation. Genes Dev 15:2642–2647.

Briscoe J, Sussel L, Serup P, Hartigan-O'Connor D, Jessell TM, Rubenstein JL, Ericson J (1999) Homeobox gene Nkx2.2 and specification of neuronal identity by graded Sonic hedgehog signalling. Nature 398:622–627.

Casarosa S, Fode C, Guillemot F (1999) Mash1 regulates neurogenesis in the ventral telencephalon. Development 126:525–534.

Chandrasekhar A (2004) Turning heads: development of vertebrate branchiomotor neurons. Dev Dyn 229:143–161.

Dubreuil V, Hirsch MR, Pattyn A, Brunet JF, Goridis C (2000) The Phox2b transcription factor coordinately regulates neuronal cell cycle exit and identity. Development 127:5191–5201.

Dubreuil V, Hirsch MR, Jouve C, Brunet JF, Goridis C (2002) The role of Phox2b in synchronizing pan-neuronal and type-specific aspects of neurogenesis. Development 129:5241–5253.

Ericson J, Thor S, Edlund T, Jessell TM, Yamada T (1992) Early stages of motor neuron differentiation revealed by expression of homeobox gene Islet-1. Science 256:1555–1560.

Fan CM, Kuwana E, Bulfone A, Fletcher CF, Copeland NG, Jenkins NA, Crew S, Martinez S, Puelles L, Rubenstein JLR, Tessier-Lavigne M (1996) Expression patterns of two murine homologs of *Drosophila* single-minded suggest possible roles in embryonic patterning and in the pathogenesis of Down syndrome. Mol Cell Neurosci 7:1–16.

Fode C, Ma Q, Casarosa S, Ang SL, Anderson DJ, Guillemot F (2000) A role for neural determination genes in specifying the dorsoventral identity of telencephalic neurons. Genes Dev 14:67–80.

Gaiano N, Nye JS, Fishell G (2000) Radial glial identity is promoted by Notch1 signaling in the murine forebrain. Neuron 26:395–404.

Garel S, Garcia-Dominguez M, Charnay P (2000) Control of the migratory pathway of facial branchiomotor neurones. Development 127:5297–5307.

Guillemot F, Lo LC, Johnson JE, Auerbach A, Anderson DJ, Joyner AL (1993) Mammalian achaete-scute homolog 1 is required for the early development of olfactory and autonomic neurons. Cell 75:463–476.

Hatakeyama J, Tomita K, Inoue T, Kageyama R (2001) Roles of homeobox and bHLH genes in specification of a retinal cell type. Development 128:1313–1322.

Hatakeyama J, Bessho Y, Katoh K, Ookawara S, Fujioka M, Guillemot F, Kageyama R (2004) Hes genes regulate size, shape and histogenesis of the nervous system by control of the timing of neural stem cell differentiation. Development 131:5539–5550.

Hirata H, Tomita K, Bessho Y, Kageyama R (2001) Hes1 and Hes3 regulate maintenance of the isthmic organizer and development of the mid/hindbrain. EMBO J 20:4454–4466.

Hirsch MR, Tiveron MC, Guillemot F, Brunet JF, Goridis C (1998) Control of noradrenergic differentiation and Phox2a expression by MASH1 in the central and peripheral nervous system. Development 125:599–608.

Hitoshi S, Alexson T, Tropepe V, Donoviel D, Elia AJ, Nye JS, Conlon RA, Mak TW, Bernstein A, van der Kooy D (2002) Notch pathway molecules are essential for the maintenance, but not the generation, of mammalian neural stem cells. Genes Dev 16:846–858.

Horton S, Meredith A, Richardson JA, Johnson JE (1999) Correct coordination of neuronal differentiation events in ventral forebrain requires the bHLH factor MASH1. Mol Cell Neurosci 14:355–369.

Inoue T, Hojo M, Bessho Y, Tano Y, Lee JE, Kageyama R (2002) Math3 and NeuroD regulate amacrine cell fate specification in the retina. Development 129:831–842.

Kageyama R, Nakanishi S (1997) Helix-loop-helix factors in growth and differentiation of the vertebrate nervous system. Curr Opin Genet Dev 7:659–665.

Lee JE (1997) Basic helix-loop-helix genes in neural development. Curr Opin Neurobiol 7:13–20.

Marshall H, Nonchev S, Sham MH, Muchamore I, Lumsden A, Krumlauf R (1992) Retinoic acid alters hindbrain Hox code and induces transformation of rhombomeres 2/3 into a 4/5 identity. Nature 360:737–741.

McKay IJ, Lewis J, Lumsden A (1997) Organization and development of facial motor neurons in the kreisler mutant mouse. Eur J Neurosci 9:1499–1506.

Morrow EM, Furukawa T, Lee JE, Cepko CL (1999) NeuroD regulates multiple functions in the developing neural retina in rodent. Development 126:23–36.

Müller M, Jabs N, Lorke DE, Fritzsch B, Sander M (2003) Nkx6.1 controls migration and axon pathfinding of cranial branchio-motoneurons. Development 130:5815–5826.

Ohtsuka T, Ishibashi M, Gradwohl G, Nakanishi S, Guillemot F, Kageyama R (1999) Hes1 and Hes5 as notch effectors in mammalian neuronal differentiation. EMBO J 18:2196–2207.

Parras CM, Schuurmans C, Scardigli R, Kim J, Anderson DJ, Guillemot F (2002) Divergent functions of the proneural genes Mash1 and Ngn2 in the specification of neuronal subtype identity. Genes Dev 16:324–338.

Pattyn A, Morin X, Cremer H, Goridis C, Brunet JF (1997) Expression and interactions of the two closely related homeobox genes Phox2a and Phox2b during neurogenesis. Development 124:4065–4075.

Pattyn A, Hirsch M, Goridis C, Brunet JF (2000) Control of hindbrain motor neuron differentiation by the homeobox gene Phox2b. Development 127:1349–1358.

Pattyn A, Vallstedt A, Dias JM, Sander M, Ericson J (2003a) Complementary roles for Nkx6 and Nkx2 class proteins in the establishment of motoneuron identity in the hindbrain. Development 130:4149–4159.

Pattyn A, Vallstedt A, Dias JM, Samad OA, Krumlauf R, Rijli FM, Brunet JF, Ericson J (2003b) Coordinated temporal and spatial control of motor neuron and serotonergic neuron generation from a common pool of CNS progenitors. Genes Dev 17:729–737.

Pattyn A, Simplicio N, van Doorninck JH, Goridis C, Guillemot F, Brunet JF (2004) Ascl1/Mash1 is required for the development of central serotonergic neurons. Nat Neurosci 7:589–595.

Ross SE, Greenberg ME, Stiles CD (2003) Basic helix-loop-helix factors in cortical development. Neuron 39:13–25.

Schuurmans C, Armant O, Nieto M, Stenman JM, Britz O, Klenin N, Brown C, Langevin LM, Seibt J, Tang H, Cunningham JM, Dyck R, Walsh C, Campbell K, Polleux F, Guillemot F (2004) Sequential phases of cortical specification involve Neurogenin-dependent and -independent pathways. EMBO J 23:2892–2902.

Sun T, Pringle NP, Hardy AP, Richardson WD, Smith HK (1998) Pax6 influences the time and site of origin of glial precursors in the ventral neural tube. Mol Cell Neurosci 12:228–239.

Taber Pierce E (1973) Time and origin of neurons and in the brain stem of the mouse. Prog Brain Res 40:53–65.

Tiveron MC, Pattyn A, Hirsch MR, Brunet JF (2003) Role of Phox2b and Mash1 in the generation of the vestibular efferent nucleus. Dev Biol 260:46–57.

Tomita K, Moriyoshi K, Nakanishi S, Guillemot F, Kageyama R (2000) Mammalian achaete-scute and atonal homologs regulate neuronal versus glial fate determination in the central nervous system. EMBO J 19:5460–5472.